



# Biomimetic liposomes and planar supported bilayers for the assessment of glycodendrimeric porphyrins interaction with an immobilized lectin

A. Makky<sup>a,b,f</sup>, J.P. Michel<sup>a,b,f</sup>, Ph. Maillard<sup>c,d,e,f</sup>, V. Rosilio<sup>a,b,f,\*</sup>

<sup>a</sup> Univ Paris-Sud 11, UMR 8612, Laboratoire de Physico-chimie des Surfaces, 5 rue Jean-Baptiste Clément, F-92296 Châtenay-Malabry, France

<sup>b</sup> CNRS, UMR 8612, F-92296 Châtenay-Malabry, France

<sup>c</sup> Institut Curie, Centre de Recherche, Bât 110-112, F-91405, Orsay, France

<sup>d</sup> CNRS, UMR 176, F-91405 Orsay, France

<sup>e</sup> Univ Paris-Sud 11, centre universitaire, F-91405 Orsay, France

<sup>f</sup> CNRS GDR 3049 PHOTOMED, France

## ARTICLE INFO

### Article history:

Received 19 October 2010

Received in revised form 18 November 2010

Accepted 22 November 2010

Available online 1 December 2010

### Keywords:

PDT

Retinoblastoma

Glycoconjugated porphyrins

Supported planar bilayer

Liposome

Lectin–sugar interaction

## ABSTRACT

Photodynamic therapy is a potentially efficient treatment for various solid tumours, among which retinoblastoma. Its efficacy depends on the preferential accumulation of photosensitizers in the malignant tissues and their accessibility to light. The specificity of drugs for retinoblastoma cells can be improved by targeting a mannose receptor overexpressed at their surface. With the aim of assessing the recognition of newly synthesized glycodendrimeric porphyrins by such receptors, we have built and characterized an original synthetic biomimetic membrane having similar lipidic composition to that of the retinal cell membranes and bearing Concanavalin A, as a model of the mannose receptor. The interaction of the porphyrin derivatives with liposomes and supported planar bilayers has been studied by dynamic light scattering and quartz crystal microbalance with dissipation monitoring (QCM-D). Only mannosylated porphyrins interacted significantly with the membrane model. The methodology used proved to be efficient for the selection of potentially active compounds.

© 2010 Elsevier B.V. All rights reserved.

## 1. Introduction

Photodynamic therapy (PDT) is a relatively new treatment modality for various diseases including superficial tumours such as basal cell carcinomas of the skin, head and neck tumours as well as tumours accessible to endoscopy like oesophageal and lung cancers [1]. Moreover, due to its therapeutic efficacy and its fewer side effects compared to chemotherapy and radiotherapy, this technique would be considered as one of retinoblastoma alternative treatments [2–5]. PDT involves a nontoxic photosensitizing agent that is activated by light at an appropriate wavelength generally in the presence of oxygen. This results in the release of organic radicals or reactive oxygen species (ROS), especially singlet oxygen that oxidize the target tissue, lead to irreversible damage and consecutive cell death (necrosis, apoptosis or autophagy) [6]. However, because of its short half life ( $\sim 4 \mu\text{s}$ ), singlet oxygen induces photodamage in its immediate vicinity only [7]. Therefore, the phototoxicity efficiency is highly

dependent upon photosensitizers' intracellular accumulation and subcellular localization [7].

Most photosensitizers used for both experimental and clinical studies in PDT are porphyrin-based compounds with a macrocyclic core providing the required photoactivity, and peripheral substituents controlling drug biodistribution and pharmacokinetics [8]. However, these compounds are usually poorly water-soluble molecules, and tend to form aggregates in aqueous solution [9–11]. Hence, to improve the efficacy of porphyrins photodynamic activity, many authors have used the glycoconjugation strategy as a potential effective way to (i) increase drug water solubility by modifying macrocycles amphipathy [12–19], and (ii) target lectin-like receptors over-expressed in some types of malignant cells [20,21] such as retinoblastoma cells [20–23]. With this aim, Ballut et al. [22,24] have recently synthesized new glycodendrimeric porphyrins as drugs with higher specificity in the treatment of retinoblastoma by PDT. The specific receptors overexpressed at the surface of cells have not been identified yet, but it is known that they are receptors to mannose and galactose [13,22,23].

Because membranes are considered as primary targets of cell photodamage for most photosensitizers used in PDT [25], studying the mechanisms of porphyrin–cell membrane interaction is of great interest. The elaboration of biomimetic membrane models mimicking the *in vivo* situation would account for a real progress allowing better

**Abbreviations:** PDT, photodynamic therapy;  $\alpha$ -MMP, methyl  $\alpha$ -D-mannopyranoside; Con A, Concanavalin A; QCM-D, Quartz crystal microbalance with dissipation monitoring; DLS, dynamic light scattering; SPB, supported planar bilayer

\* Corresponding author. Univ Paris-Sud 11, UMR 8612, Laboratoire de Physico-chimie des Surfaces, 5 rue Jean-Baptiste Clément, F-92296 Châtenay-Malabry, France.

E-mail address: [veronique.rosilio@u-psud.fr](mailto:veronique.rosilio@u-psud.fr) (V. Rosilio).

comprehension of these mechanisms. Many research groups have already used different organized systems, such as monolayers [26,27] or liposomes [28–37] for modeling a cell membrane and studying porphyrin interaction with it. However, these model systems containing a single lipid or even a binary lipid mixture were not biomimetic enough of cancerous cell membranes, and they lacked the lectin-like receptors at their surface. In a previous work, we have focused on the non-specific interactions and penetration ability of glycodendrimeric porphyrins into mixed phospholipid monolayers and liposome bilayers having similar lipidic composition to that of the retinoblastoma cell membranes [38–41], with increasing cholesterol content from 10 to 30 mol% [42]. We have shown that cholesterol changes in retinoblastoma cell membranes did not modify the penetration ability of the studied porphyrins. Moreover, we have demonstrated that glycoconjugation of porphyrins reinforced their amphiphathy and promoted their interaction with those membranes [42]. In a more recent work, we have analyzed more specifically the ability of the porphyrin derivatives to be recognized by a mannose-specific protein, Concanavalin A, mimicking some of the receptors over-expressed at the surface of retinoblastoma cells [22,43]. Our results showed that only mannosylated porphyrins could specifically interact with Concanavalin A (Con A), and that the spacer length between a porphyrin core and its mannose moieties played a crucial role in this interaction. To avoid non-specific interactions with the lipids, Con A has been studied alone, free in the aqueous medium or immobilized onto a SAM-functionalized QCM-D gold sensor.

Herein, we have built and characterized liposomes and supported planar bilayers having a similar lipidic composition to that of retinoblastoma cell membranes as previously described [42], on which Con A has been grafted. This more complete model allowed us to better mimic the *in vivo* conditions and to get a better insight into the mechanisms of interaction between glycoconjugated porphyrins and retinoblastoma cells at a pH of 6.5, close to that reported for tumorous tissues [44].

## 2. Materials and methods

### 2.1. Chemicals

The glycodendrimeric porphyrins compound **1** (Mw = 1692.81 g/mol) and compound **2** (Mw = 1823.8 g/mol) were prepared as described previously by Ballut et al. [22,24]. They were tri-mannosylated with a DEG (diethylene glycol) and a TEG (triethylene glycol) spacer, respectively. We also studied a non-glycoconjugated porphyrin (compound **1c**, Mw = 1236.09 g/mol) [24], which had the same structure as compound **1**, except for the mannose residues replaced by OH groups. This non-glycoconjugated compound was considered as a control for compound **1** and to a lower extent for compound **2**. The three porphyrin derivatives were poorly soluble in water but soluble in a (9:1 v/v) mixture of chloroform/methanol used for liposome preparation. Their chemical structures are presented in Fig. 1.

The phospholipids used for building the biomimetic membrane: 1-stearoyl-2-oleoyl-*sn*-glycero-3-phospho-L-serine (sodium salt) (SOPS, Mw = 812.05 g/mol), 1-stearoyl-2-oleoyl-*sn*-glycero-3-phosphocholine (SOPC, Mw = 788.14 g/mol), 1-stearoyl-2-oleoyl-*sn*-glycero-3-phosphoethanolamine (SOPE, Mw = 746.06 g/mol) and 1,2-dioleoyl-*sn*-glycero-3-phosphoethanolamine-N-(glutaryl) (sodium salt) (DOPE-glutaryl, Mw = 880.12 g/mol) were purchased from Instruchemie (Delfzijl, The Netherlands). They were 99% pure and were used without any further purification. Concanavalin A (Type IV, Mw: 25500 g/mol per monomer), Sepharose 4B gel, methyl  $\alpha$ -D-mannopyranoside ( $\geq 99\%$  pure, Mw = 194.18 g/mol), mannan from *Saccharomyces cerevisiae* ( $\geq 95\%$  pure), 1,2-dimyristoyl-*sn*-glycero-3-phosphocholine (DMPC, 99% pure, Mw = 677.93 g/mol), cholesterol (CHOL, 99% pure, Mw = 386.66 g/mol), HEPES (99.5% pure, Mw = 238.31 g/mol), sodium chloride (NaCl, 99% pure,

Mw = 58.44 g/mol), calcium chloride ( $\text{CaCl}_2 \cdot 2\text{H}_2\text{O}$ , 98% pure, Mw = 147.02 g/mol), nickel chloride ( $\text{NiCl}_2 \cdot 6\text{H}_2\text{O}$ , 98% pure Mw = 237.69 g/mol), 1-ethyl-3-[3-(dimethylamino)propyl] carbodiimide hydrochloride (EDC), N-hydroxysuccinimide (NHS), ethanolamine (99.5% pure, Mw = 61.08 g/mol) and glutaraldehyde (25% in  $\text{H}_2\text{O}$ , Mw = 100.12 g/mol) were purchased from Sigma (Saint-Louis, USA). Sodium acetate NORMAPUR™ AR ( $\text{CH}_3\text{COONa}$ , Mw = 82.03 g/mol) was purchased from VWR Prolabo (Briare, France). Chloroform and methanol (99% pure) provided by Merck (Germany) were analytical grade reagents. Ultrapure water ( $\gamma = 72.2$  mN/m at 22 °C) produced by a Millipore Synergy 185 apparatus coupled with a RiOs5™ with a resistivity of 18.2 M $\Omega$ .cm was used in all experiments. All glassware were soaked for an hour in a freshly prepared TFD4 (Franklab) detergent solution (15% v/v), then abundantly rinsed with milli-Q water and finally oven-dried.

### 2.2. Methods

#### 2.2.1. Preparation of liposomes for porphyrin solubilization, Con-A coupling, and supported bilayer formation

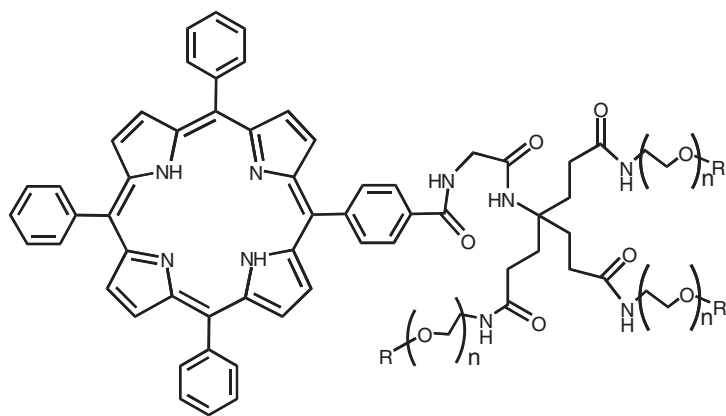
Liposomes were prepared according to Bangham's method followed by the extrusion of vesicles suspensions [45–47]. In brief, phospholipid solutions in chloroform/methanol (9:1 v/v) were evaporated for 3 hours under reduced pressure, and the resulting dry lipid film was hydrated by the corresponding buffer to achieve the desired concentration. The lipid suspension thus obtained was then extruded 15 times through a 200 nm polycarbonate membrane at 50 °C for DMPC liposomes and 60 °C for the others (Avestin Lipofast extruder, Ottawa, California).

In this work, 3 types of liposomes having different lipid compositions have been used:

- (i) Liposomes of DMPC bearing porphyrins (500:1 molar ratio) at 2 mM were prepared as previously described [22]. In brief, DMPC and a porphyrin were solubilized in a (9:1) chloroform–methanol mixture. After complete evaporation of the organic solvents in a rotatory evaporator under reduced pressure, the resulting dry film was hydrated by HEPES buffer (HEPES 10 mM, 150 mM NaCl, pH 6.5) with divalent ions (1 mM  $\text{Ca}^{2+}$  and 1 mM  $\text{Ni}^{2+}$ ). The divalent cations were required for Con A activity [48] and the pH was chosen to match that reported in cancer tissues. These liposomes were meant to “solubilise” and carry the porphyrins toward their target.
- (ii) 10 mM liposomes formed of SOPC, SOPE, SOPS and cholesterol (4.5:3.5:1:1 molar fractions) in HEPES buffer (10 mM HEPES, 150 mM NaCl, pH 7.4). Concanavalin A was then grafted onto the surface of these liposomes for studying their interaction as models of the retinoblastoma cell membrane, with porphyrin-bearing DMPC vesicles.
- (iii) 2 mM carboxylated liposomes (SOPC/DOPE-glutaryl/SOPS/CHOL: 4.5:3.5:1:1 molar fractions) for the formation of planar bilayers onto the  $\text{SiO}_2$  surface of the QCM-D sensor, and subsequent coupling of Con A. These liposomes were prepared in sodium acetate buffer (10 mM sodium acetate, 150 mM NaCl, pH = 4) to facilitate their adsorption onto the  $\text{SiO}_2$  surface, by avoiding electrostatic repulsion with the negative charge of COOH moieties at higher pH.

#### 2.2.2. Conjugation of Concanavalin A to SOPC/SOPE/SOPS/CHOL liposomes

Con A immobilization onto the surface of liposomes was achieved according to the method described by Nakano et al. [49] and Liu et al. [50] with some modifications. Briefly, 1 ml of SOPC/SOPE/SOPS/CHOL liposomes was added slowly (10  $\mu\text{l}/\text{min}$ ) to 0.6 ml of 5% aqueous glutaraldehyde solution with gentle stirring for 1 hour at 4 °C. Glutaraldehyde in excess was removed by dialysis (MWCO 15 kDa) overnight at 4 °C. Then 0.2 ml of a Con A solution (10 mg/ml in HEPES,



**Compound 1c**      **Compound 1**      **Compound 2**  
 $n = 2$                        $n = 2$                        $n = 3$   
 $R = H$                        $R = \alpha\text{-mannose}$        $R = \alpha\text{-mannose}$

**Fig. 1.** Chemical structures of the studied porphyrins.

pH 7.4) was added under gentle stirring at 4 °C. After 1 hour of incubation, 0.5 M ethanolamine-HCl (0.2 ml, pH 7.4) was added to liposomes to block excess aldehyde groups on the liposomes surface. The system was left for 1 hour at 4 °C.

The Con A-conjugated liposomes thus obtained were separated from uncoupled Con A by gel permeation chromatography on Sepharose 4B columns with HEPES buffer (HEPES 10 mM, NaCl 150 mM, pH 7.4) as eluent. The elution profiles of Con A and the liposomes were monitored using the BCA™ Protein Assay (Sigma St. Louis, USA) and phospholipid assay kit (Diagnostics Partners, France). Samples of the eluted fractions (2 ml) were collected and analyzed using a CARY 100 Bio UV-visible spectrophotometer (Varian, USA) at 562 and 500 nm for protein and lipid assays, respectively.

#### 2.2.3. Vesicle size and zeta potential measurements:

The analysis of the size and zeta potential ( $\zeta$ ) of the liposomes was carried out at 25 °C using a Zeta-sizer (Nano ZS90, Malvern). The  $\zeta$  measurements were performed after redispersion of 50  $\mu$ l of 4 mM liposomes in HEPES buffer at pH 6.5 in 1 ml of deionised water. Dilution had no effect on liposome size.

#### 2.2.4. Liposomes aggregation assay with immobilized Con A

To verify that the specific activity of Con A was maintained when it was coupled to liposomes, we have performed a similar aggregation assay to that of Chen et al. [51] using mannan, a Con A polyvalent substrate. In this assay, 200  $\mu$ l of a mannan solution (1 mg/ml in HEPES buffer (10 mM HEPES, 150 mM NaCl, 1 mM  $\text{CaCl}_2 \cdot 2\text{H}_2\text{O}$  and 1 mM  $\text{NiCl}_2 \cdot 6\text{H}_2\text{O}$ , pH 6.5) was added to 500  $\mu$ l of fresh Con A-liposomes (2 mM) saturated (or not) beforehand with methyl  $\alpha$ -D-mannopyranoside ( $\alpha$ -MMP), a substrate with a high affinity to Con A [52]. Con A activity was considered as preserved if no liposome aggregation occurred when Con A specific sites were saturated with  $\alpha$ -MMP. The mixture was vortexed for 10 min and incubated for 1 hour at room temperature. Vesicles diameters were measured before and after addition of mannan using the Zetasizer. All measurements were carried out at 25 °C.

#### 2.2.5. Formation of a Con A conjugated-planar lipid bilayer

Experiments using the quartz crystal microbalance with dissipation monitoring were performed with a QCM-D E4 (Q-Sense, Gothenburg, Sweden). The QCM-D sensor allows the measurement of the oscillation frequency shift ( $\Delta f$ ) of a quartz crystal and simultaneous energy

dissipation change ( $\Delta D$ ). Whereas changes in resonance frequency are related to the mass of the material adsorbed on or removed from the sensor, changes in energy dissipation provide information on the viscoelastic properties of the adsorbed material. AT-cut  $\text{SiO}_2$ -coated quartz crystals with a fundamental frequency of 5 MHz were provided by Q-Sense AB. These crystals were stored in 10 mM sodium dodecyl sulfate (SDS) solution between measurements. Prior to their use, they were thoroughly rinsed with ultrapure water, dried under a  $\text{N}_2$  stream and treated in an UV-ozone chamber for 20 min.

A supported planar bilayer (SPB) was easily obtained by spreading and then spontaneous breaking of phospholipid-cholesterol vesicles onto the  $\text{SiO}_2$  quartz. However, it was not possible to subsequently graft the lectin onto this SPB by *in situ* activation of the phosphatidylethanolamine (PE) headgroups by glutaraldehyde, as described for the Con A-conjugated liposomes. Indeed, the addition of glutaraldehyde probably created a network between free PE headgroups, hindering Con A grafting to the surface. The alternative method consisted in replacing SOPE in the liposomes formulation by DOPE-glutaryl, a commercially available phospholipid derivative. As such, PE groups were already activated and presented a free COOH group for Con A coupling. Lectin immobilization on the preformed supported bilayer was further achieved by conversion of the carboxylic acid functions of DOPE-glutaryl into *N*-hydroxysuccinimide esters by reaction with *N*-hydroxysuccinimide (NHS) in the presence of a water-soluble carbodiimide (EDC), followed by reaction with Con A.

### 3. Results

#### 3.1. Elution profiles of Con A-conjugated liposomes

After conjugation, Con A-bearing liposomes were separated from the unbound lectin by gel permeation chromatography, and the various fractions were analyzed. As shown in Fig. 2a, the free Con A was collected in one peak. This result is consistent with the elution profile described by Santos et al. [53] for this lectin. When Con A was incubated with pre-activated liposomes, its elution profile drastically changed and two peaks of Con A were observed (Fig. 2b). The first one appeared in the fourth fraction, in which liposomes were totally eluted, and the second one in the eighth fraction, corresponding to the unbound Con A.

Using the immobilization procedure, lectin-liposome conjugates were obtained with a lectin/lipid molar ratio of  $6.7 \pm 1.0 \times 10^{-4}$ , in good agreement with those (up to  $5 \times 10^{-4}$ ) obtained by Bogdanov et al. [54]

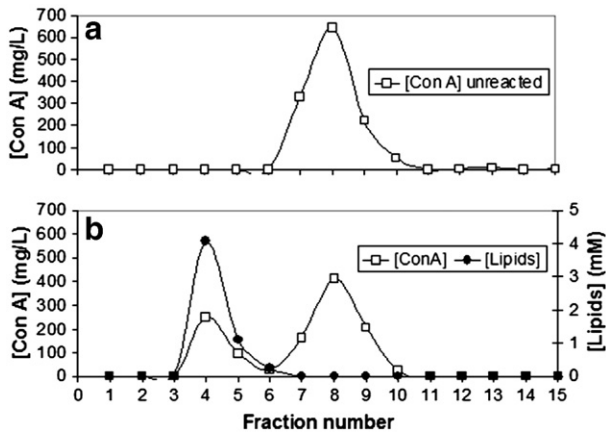


**Fig. 2.** Elution profiles for (a) the free Con A, and (b) Con A after reaction with pre-activated liposomes.

for Ricinus communis agglutinin (RCA) and wheat germ agglutinin (WGA) immobilizations onto a liposome surface, using carbodiimide chemistry [54].

### 3.2. Aggregation assay of Con A-conjugated liposomes with mannan

No liposome aggregation was observed upon addition of a mannan solution to non-conjugated liposomes. Their size measured by DLS

remained unchanged (Table 1). Conversely, addition of the polysaccharide to Con A-conjugated liposomes induced a dramatic increase in vesicles diameter accounting for their aggregation. This result proved that mannan was able to interact with the lectin immobilized onto a vesicle surface. The multiplicity of binding sites on the polysaccharide probably promoted the interaction of mannan with more than one conjugated lectin molecule, leading to liposomes bridging and formation of large aggregates. This would explain the high diameter values measured, and the bimodal size distribution observed for these liposomes. In the presence of  $\alpha$ -MMP, which saturated the specific sites of Con A, the addition of mannan did not induce any liposomes aggregation: their size remained unchanged. These data demonstrated the effective conjugation of Con A to the liposomes outer surface and the preservation of Con A functional binding activity to mannose moieties.

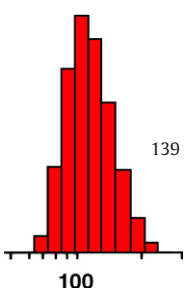
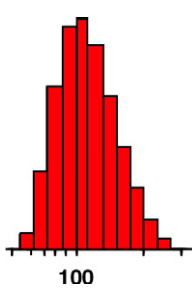
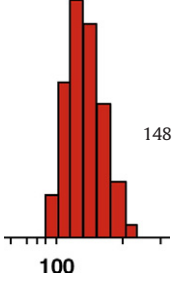
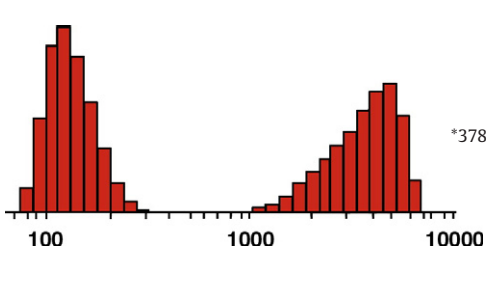
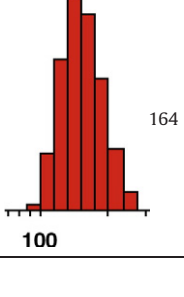
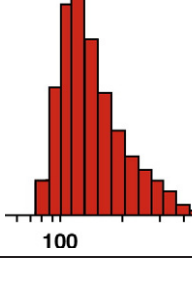
### 3.3. Zeta potential measurements

We have also evaluated the effect of Con A on the zeta potential of vesicles suspension.

Non-conjugated liposomes and free Con A exhibited zeta potential values of  $-64.5 \pm 2.3$  mV and  $-14.2 \pm 0.3$  mV, respectively (Table 2). When free Con A was mixed with unmodified liposomes in the buffer solution, no significant change in zeta potential was observed ( $-62.2 \pm 2.5$  mV). Conversely, when the lectin was grafted to liposomes surface, the zeta potential was significantly lowered to  $-79.4 \pm 2.5$  mV. This result is consistent with the effective grafting of Con A to the surface of liposomes, making it more negatively charged than the unmodified

**Table 1**

Liposome diameters before and following addition of 200  $\mu$ l of a 1 mg/ml mannan solution to 2 mM of unmodified liposomes, Con A-conjugated liposomes and Con A-conjugated liposomes saturated with  $\alpha$ -MMP.

Liposomes	Before mannan addition		After mannan addition	
	Diameter (nm)	Volume (%)	Diameter (nm)	Volume (%)
SOPC/SOPE/SOPS/CHOL	 100	139	100	 100
Liposomes-Con A	 100	148	100	 100      1000      10000 *3780      *48.3
Liposomes-Con A saturated with $\alpha$ -MMP	 100	164	100	 100



**Table 2**Zeta potential ( $\zeta$ ) values for liposomes and Con A samples.

Liposomes	Zeta (mV)
Non conjugated liposomes	$-66.8 \pm 2.9$
Free Con A	$-14.2 \pm 0.3$
Con A-conjugated liposomes	$-79.4 \pm 2.5$
Con A mixed with liposomes	$-62.2 \pm 2.5$

liposomes. A similar result has been reported by Santos et al. [53] with doxorubicin-loaded Con A-liposomes.

### 3.4. Interaction of porphyrin-bearing DMPC vesicles with Con A-conjugated SOPC/SOPE/SOPS/CHOL liposomes

In a previous work [22], we have shown that compounds **1c**, **1** and **2** could be solubilised into the bilayer of DMPC liposomes. The liposomes bearing mannosylated porphyrins were able to interact significantly with free Con A through the outward exposure of their mannose moieties into the aqueous phase. Herein we have studied the ability of these porphyrin-loaded liposomes to interact with Con A immobilized onto SOPC-SOPE-SOPS-CHOL liposomes surfaces, mimicking more efficiently the *in vivo* conditions than did the free Con A in solution.

The size of Con A-conjugated liposomes was not significantly affected by the addition of DMPC-compound **1c** vesicles (148 nm versus 157 nm). Conversely, after adding DMPC-compound **1** and DMPC-compound **2** liposomes, a dramatic increase in vesicles diameter was observed with emergence of new vesicle families having a diameter of about 5000 nm (Table 3). This striking result demonstrates that mannosylated porphyrins borne by DMPC liposomes were able to interact specifically with multiple Con A-conjugated liposomes, leading to the formation of liposome aggregates (Fig. 3), even if Con A was immobilized onto the vesicles surface at a low density (Con A was grafted to superficial PE head groups only). However, no significant

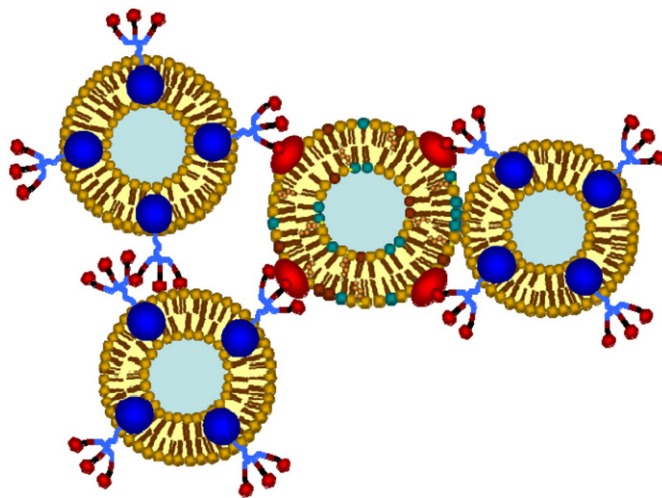


**Fig. 3.** schematic representation of aggregates formation following mixing mannosylated porphyrin-bearing vesicle and Con A-conjugated liposome suspensions.

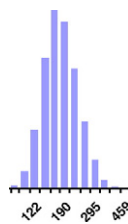
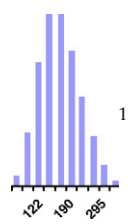
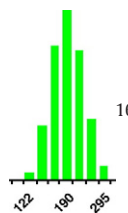
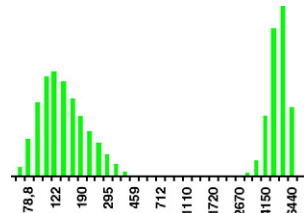
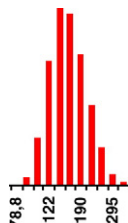
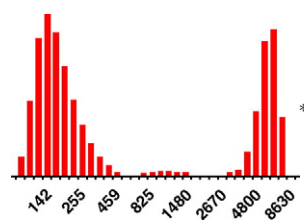
difference in the aggregates size between DMPC-compound **1** and DMPC-compound **2** liposomes could be drawn, because the obtained values were beyond the detection limits of the DLS apparatus. The influence of the spacer length was thus not apparent from these measurements.

### 3.5. Formation of a biomimetic supported planar bilayer (SOPC/SOPS/CHOL/DOPE-glutaryl)

Solid-supported membranes are widely used as well-defined model systems for fundamental biophysical research and have been

**Table 3**

DLS measurements of Con A-conjugated liposomes size before and after addition of porphyrin-bearing liposomes.

Liposomes	Before interaction with Con A-conjugated liposomes 148 nm (100%)		After interaction with Con A-conjugated liposomes 148 nm (100%)			
Composition	Diameter (nm)	Volume (%)	Diameter (nm)	Volume (%)		
DMPC compound 1c		146	100		157	100
DMPC compound 1		160	100		*5180	*35.6
DMPC compound 2		161	100		*5090	*33.6

proposed as biomimetic surfaces to elucidate the physical behaviour of cell membranes [55] and membrane-bound macromolecules [56]. To create supported planar bilayers, a multitude of methods has been proposed, including Langmuir–Blodgett techniques [57,58] and spreading of vesicles on various preconditioned supports [55,59–63]. In this work, we have used the latter approach by spreading small lipid vesicles onto hydrophilic solid  $\text{SiO}_2$  substrates (Fig. 4).

Fig. 4a shows the process of planar bilayer formation on the  $\text{SiO}_2$  quartz followed by QCM-D measurement at the third overtone (15 MHz). After injection of the 2 mM COOH-liposome suspension, the frequency decreased (**1**, mass uptake) and simultaneously the dissipation increased (indicating that the film became more viscous) until a critical density of adsorbed intact vesicles was reached. This critical density of vesicles relates to the minimum in frequency ( $\sim -53$  Hz) and the maximum in dissipation ( $7.5 \times 10^{-6}$ ). At this point, and as described by many authors [59,64], the vesicle rupture usually starts. Following this rupture onto the quartz surface,  $\Delta f$  increased (**2**), indicating a mass loss, and  $\Delta D$  decreased accounting for the presence of a more rigid adsorbed film. Finally (**3**),  $\Delta f$  and  $\Delta D$  curves stabilized at  $\Delta f \sim -25.3$  Hz and  $\Delta D \sim 0.2 \times 10^{-6}$ , and no significant change in the baseline was observed upon rinsing with HEPES buffer (arrows in Fig. 4a). This result demonstrated the formation of a stable supported planar bilayer (SPB). Indeed, the  $\Delta f$  and  $\Delta D$  values corresponding to the breaking of COOH-liposomes fully matched those reported for a complete homogeneous supported planar bilayer ( $\Delta f \sim -26$  Hz and  $\Delta D \sim 0.3 \times 10^{-6}$ ) [61,64–66]. Moreover the final low dissipation shift ( $\Delta D \sim 0.2 \times 10^{-6}$ ) attested the good quality of the supported bilayer formed [62].

The  $\Delta f$ – $\Delta D$  plot in Fig. 4b allows discarding time as an explicit parameter and highlights the mechanistic details of bilayer formation following liposomes deposition. After a simultaneous  $\Delta f$  decrease and  $\Delta D$  increase from the zero coordinate, the plot shows a cusp at  $\Delta f = -52.3$  Hz and  $\Delta D \sim 7.8 \times 10^{-6}$ . This cusp corresponds to maximal liposome adsorption. The following phase of vesicles rupture is indicated by the simultaneous  $\Delta f$  increase and  $\Delta D$  decrease, until they both reach stable values. Similar plots have been obtained by many authors describing supported bilayer formation [61,65].

### 3.6. Con A immobilization onto the phospholipid-cholesterol planar bilayers

The time-dependent frequency and dissipation shifts were recorded during Con A immobilization on the supported planar bilayer (Fig. 5). At  $t = 20$  min after SPB formation, the Con A solution was injected into the QCM-D cell. This induced a decrease of the crystal resonance frequency below  $-40$  Hz and a simultaneous  $\Delta D$  increase up to  $12 \times 10^{-6}$ , corresponding to the adsorption of a viscous layer of Con A onto the bilayer surface. Three rinsing steps were applied as shown by the arrows in Fig. 5, first with HEPES buffer to eliminate weakly bound Con A then one with the ethanolamine solution to inactivate the free glutaryl groups. Finally the cell was rinsed with HEPES buffer and the measured  $\Delta f$  and  $\Delta D$  signals were only slightly affected, indicating that the covalently bound Con A molecules remained firmly attached to the bilayer surface. The obtained final values were  $\Delta f \sim -36.7$  Hz and  $\Delta D \sim 10.6 \times 10^{-6}$ .

### 3.7. Interactions of porphyrin-bearing DMPC liposomes with the biomimetic Con A-conjugated supported bilayer

After formation onto the quartz surface of a planar biomimetic bilayer with similar lipidic composition to that of the retinoblastoma cell membrane [42], with Con A-mimicking the sugar receptor-covalently bound to the upper leaflet, we have injected under flow conditions DMPC-compound **1c**, DMPC-compound **1** and DMPC-compound **2** liposomes into the measurement cell. Fig. 6 shows the following evolution of  $\Delta f$  and  $\Delta D$  as a function of time.

As shown in Fig. 6, whatever the composition of the liposomes injected into the QCM-D measurement cell, variations in  $\Delta f$  and  $\Delta D$  signals were always observed. In all cases, a quasi steady state was reached after 20 to 30 min. The immediate decrease in resonant frequency can be explained by the increased effective mass onto the QCM-D sensor, due to vesicles adsorption. A simultaneous increase in energy dissipation would indicate a more viscous behaviour as more liposomes were adsorbed onto the bilayer. However, the amplitudes of the signals appeared highly dependent on the porphyrin derivative embedded into the DMPC liposomes bilayer. Upon injection, vesicles bearing mannosylated porphyrins induced the highest magnitudes of

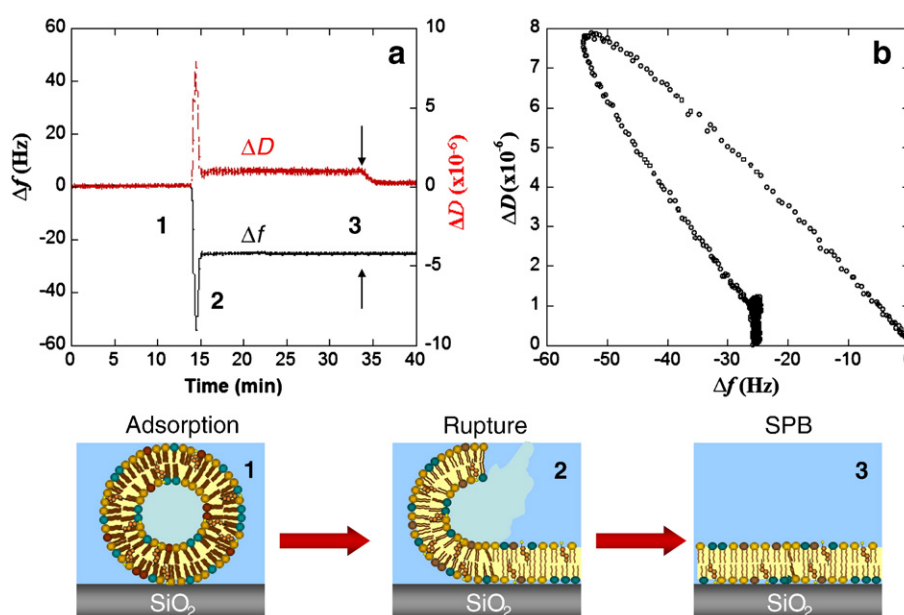


Fig. 4. Deposition and rupture of COOH-liposomes onto the  $\text{SiO}_2$  surface ([lipids] = 2 mM in acetate buffer, at pH = 4, vesicles size  $\sim 146$  nm): (a)  $\Delta f$  and  $\Delta D$  change with time at 15 MHz; Arrows indicate buffer rinsing. (b) Dissipation vs. frequency shift.

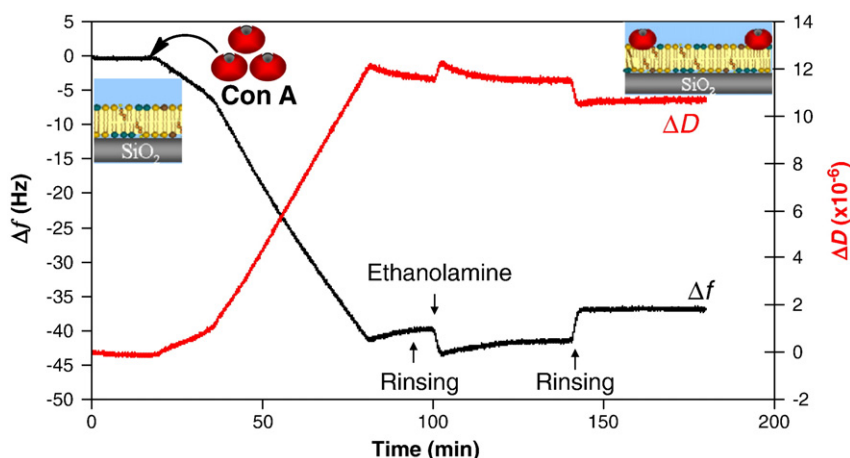


Fig. 5.  $\Delta f$  and  $\Delta D$  ( $n = 11$ ) following Con A immobilization onto activated COOH-supported planar bilayer by EDC/NHS.

$\Delta f$  and  $\Delta D$  compared to pure DMPC and compound **1c**-liposomes. A difference in frequency shift between the mannosylated porphyrin-bearing vesicles was observed only in the first part of the curve, and could be related to a different distribution of grafted Con A onto the supported planar bilayer. At equilibrium, after buffer rinsing, the glycodendrimeric porphyrin-bearing vesicles led to the same  $\Delta f$  value ( $\sim -72$  Hz), but different  $\Delta D$  ones,  $27.8$  and  $33.7 \times 10^{-6}$  for compound **1** and compound **2**, respectively. The maximal frequency shift value ( $-72 \pm 3$  Hz) was lower than that reported for the adsorption of a layer of intact liposomes, which usually ranges from  $-90$  to  $-400$  Hz, depending on liposome size and adhesion process [61,67–69]. Conversely, it was much higher than that obtained for a supported planar bilayer ( $\Delta f \sim -26$  Hz). Also, the  $\Delta D$  values were very high,  $27.8$  and  $33.7 \times 10^{-6}$  for liposomes bearing compounds **1** and **2** respectively, compared to that for a planar bilayer ( $\Delta D \sim 0.3 \times 10^{-6}$ ). Moreover, the normalized change in frequency ( $\Delta f/n$ ) and dissipation ( $\Delta D$ ) for the six overtones ( $n = 3, 5, 7, 9, 11, 13$ ) did not overlap (data not shown). This would indicate that the adsorbed liposomes formed a non-rigid incomplete layer of intact liposomes [70,71].

Conversely, for pure DMPC and compound **1c**-bearing liposomes, very small frequency and dissipation shifts were observed after their injection into the measurement cells ( $\Delta f = -5$  Hz only, and  $\Delta D = 5$  to  $6 \times 10^{-6}$ ). Moreover, the following washing step with buffer induced complete removal of the liposomes from the bilayer surface, as inferred from the evolution of the  $\Delta f$  value towards zero. The non-null  $\Delta f$  and  $\Delta D$  values measured after a single buffer rinsing could indicate the presence of residual liposomes or remains of them weakly bound to the bilayer.

To get a better insight into the mechanisms of interaction of the various populations of liposomes with the Con A-conjugated planar bilayer, we have plotted the variation of dissipation energy as a function of the frequency shift, which allowed us to analyze the relationship between changes in rigidity and added/lost mass for the various porphyrin-bearing liposome systems (Fig. 7).

The comparison between the liposomes bearing the different porphyrins clearly showed that they did not interact in the same manner with the biomimetic planar bilayer. Indeed, DMPC and compound **1c**-bearing liposomes, exhibited the highest dissipation

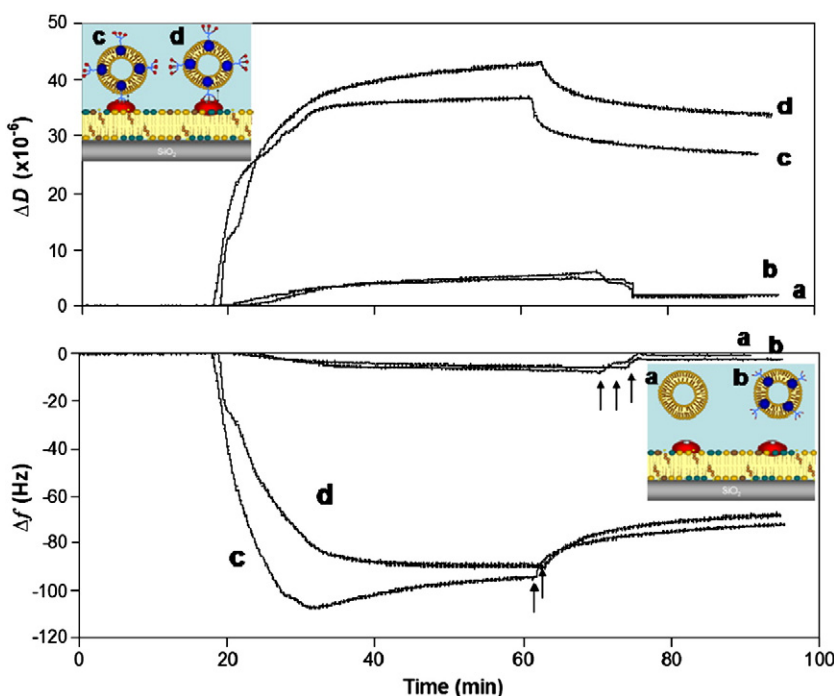
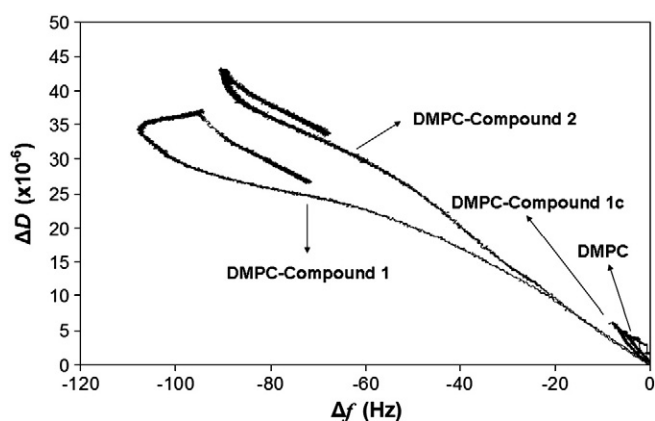


Fig. 6.  $\Delta f$  and  $\Delta D$  ( $n = 11$ ) evolution following liposomes injection into the QCM-D cell containing immobilized Con A onto the supported planar bilayer. a: pure DMPC liposomes, b: DMPC-compound **1c**, c: DMPC-compound **1**, and d: DMPC-compound **2**. Arrows indicate the times at which the electrodes were rinsed with HEPES buffer.



**Fig. 7.** Dissipation change versus frequency shift for DMPC and DMPC-porphyrin liposomes injected in the cell containing the immobilized Con A onto the planar phospholipid-cholesterol bilayer.

at a same given frequency shift ( $-5$  Hz) compared to liposomes bearing mannosylated porphyrins. Moreover, after buffer rinsing,  $\Delta f$  and  $\Delta D$  values became null. These data indicate that the liposomes were simply adsorbed onto the Con A-bilayer surface. Therefore, they could move freely during quartz crystal oscillations. Conversely, compounds **1** and **2**-bearing vesicles induced lower energy dissipation at the same frequency shift ( $-5$  Hz). These liposomes were apparently strongly bound to the bilayer, and could not move as well as DMPC or compound **1c**-bearing liposomes. Moreover, at a higher frequency shift ( $\sim -72$  Hz), liposomes bearing compound **2** showed a much higher increase in dissipation compared to those bearing compound **1**. Final parts of the curves show that most of the liposomes remained firmly bound to the bilayer despite the successive rinsing steps with buffer. This difference in behavior between liposomes bearing mannosylated porphyrins and non-mannosylated ones indicates that vesicles bearing mannosylated porphyrins were able to interact significantly with Con A covalently bound to the phospholipid-cholesterol bilayer although Con A was grafted at a low density.

Considering the small difference in spacer length between compounds **1** and **2** (only one ethylene oxide) and the similar size of all studied liposomes ( $\sim 146$  nm), superimposition of the curves in Fig. 7 for the two compounds could be expected. However, this was not the case. The discrepancy in dissipation could originate from the greater mobility of mannoside moieties provided by the longer spacers in compound **2**. DMPC-**2** liposomes would be less tightly bound to the bilayer surface and would form a more viscous layer than the DMPC-**1** ones. The spacer length would therefore play a significant role in the binding process of compound **1**- and compound **2**-bearing liposomes with the biomimetic bilayer.

### 3.8. Interactions of porphyrin-bearing DMPC liposomes with the supported bilayer devoid of Con A

To analyze the predominance of the specific interaction over the non-specific one in the adsorption process of mannosylated porphyrin-bearing liposomes to the biomimetic bilayer, we have repeated the same experiment with a planar phospholipid-cholesterol bilayer lacking the Con A. As shown in Fig. 8, only a small decrease in frequency ( $\Delta f \sim -5 \pm 1$  Hz) and short increase in dissipation ( $\Delta D \sim 5 \times 10^{-6}$ ) occurred upon injection of liposomes bearing mannosylated porphyrins. Moreover, both  $\Delta f$  and  $\Delta D$  returned to their initial values ( $\Delta f = 0$  and  $\Delta D = 0$ ) after buffer rinsing. This clearly indicates that this time, liposomes were only weakly bound to the bilayer surface.

## 4. Discussion

In this study, we have built and characterized, for the first time, a complex membrane model including three phospholipids, cholesterol, and a recognition protein, for assessing drug-membrane interactions. This membrane has been specifically built for studying the ability of glycodendrimeric porphyrins carried by DMPC liposomes to be recognized by a mannose specific receptor overexpressed at the surface of the retinoblastoma cells [43]. Prior to the analysis of the full system, we have studied the non-specific interactions of the porphyrins with the lipid bilayer without the lectin, but with increasing cholesterol content [42]. This first model showed that if the presence of cholesterol (10–30 mol%) strongly affected the viscoelastic properties of the lipid matrix, it did not particularly attract the porphyrin derivatives or hinder their penetration into the membrane. Since no difference in porphyrin penetration behaviour could be observed between lipid models with the different cholesterol contents, we chose to build our model with 10 mol% only. The reason for this choice was that the liposomes containing 30 mol% cholesterol had a very rigid membrane, and did not easily break and form a complete and homogeneous supported planar bilayer.

The study of the interaction of the glycodendrimeric porphyrins with the mono- and bilayer lipid models have shown another interesting trend: despite the absence of the recognition protein, the sugar moieties of glycoconjugated porphyrins were able to strongly interact with the mixed lipid monolayer, at the level of phospholipid headgroups. Thus, besides the expected hydrophobic interaction between the tetrapyrrolic macrocycle and phospholipid acyl chains, there was another non-specific interaction between the glycodendrimeric porphyrins and the lipids that had to be taken into account. In order to assess the purely specific interaction with the mannose-receptor, we have then used Concanavalin A, free in the aqueous medium or immobilized onto a SAM-functionalized QCM-D gold sensor [43]. We have demonstrated that the glycodendrimeric porphyrins incorporated into the bilayer of DMPC liposomes exposed their mannose moieties outwards and were able to interact specifically with the free or immobilized Concanavalin A. By comparing the behaviour of the three porphyrin derivatives in the presence of Con A and human serum albumin, we have observed that the binding of the glycodendrimeric porphyrins to Con A was mostly specific and did not merely result from hydrophobic interactions. Furthermore, we have shown that the spacer length played a crucial role in this interaction since compound **2** interacted more significantly with the lectin than compound **1**. However in this latter study, Con A was studied alone without the lipid matrix and was in large excess compared to *in vivo* conditions. This could lead to an overestimation of the strength of the specific interaction compared to the non-specific one. To achieve a more biomimetic model, we have in the present work grafted the lectin to the phospholipid-cholesterol matrix and studied the interaction of the whole model system with the various compounds. Compared to the *in vivo* system, it could have been more appropriate to incorporate the lectin into the lipid bilayer rather than graft it at the surface. Partial penetration of the protein in the membrane might be needed for optimal functionality [72]. However even after grafting, such a penetration could occur depending on the hydrophobic character of the lectin and the fluidity of the bilayer. Ramsden has shown that the fluidity of a lipid bilayer can allow protein post-binding rearrangement within the plane of the membrane [72]. We have studied the penetration of Con A into monolayers of SOPC/SOPE/SOPS/CHOL. The  $\Delta\pi$ - $\pi_i$  relationship (with  $\pi_i$ , the initial pressure of the mixed monolayer) showed that the maximum insertion pressure was 27.0 mN/m (data not shown), lower than the pressure expected in membranes (30–35 mN/m) [73]. Penetration of Con A into the bilayer after grafting seems thus unlikely. The actual receptor is still unknown, and it is unclear if it is solely a recognition protein or a real transporter [13]. It appeared, therefore, both time-



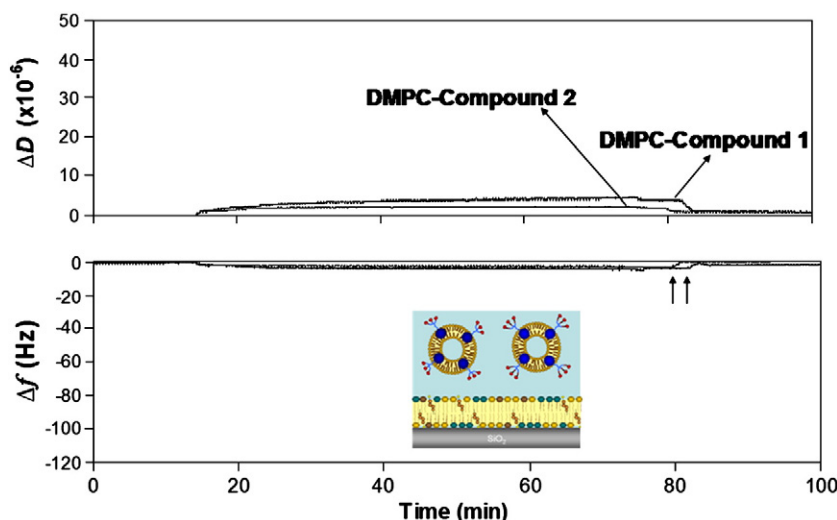


**Fig. 8.**  $\Delta f$  (a) and  $\Delta D$  (b) ( $n = 11$ ) following DMPC-compound 1 and DMPC-compound 2 liposomes injection into the QCM-D cell containing the phospholipid-cholesterol supported planar bilayer without Con A. Arrows indicate the times at which the sensors were rinsed with HEPES buffer.

consuming and useless to try to incorporate Concanavalin A into the matrix, with a risk to lose its recognition activity. Several trials have been made, however, to form mixed lipid-Con A monolayers with controlled surface density at the air–water interface that could be transferred on the  $\text{SiO}_2$  quartz surface. They were unsuccessful, because Con A was partially solubilised into the subphase. Thus, we have developed one protocol to graft the lectin to liposomes and another to conjugate it to the supported bilayer. The purpose of using the two models was to study the interaction first in conditions where the system had a certain degree of freedom (both liposome systems being mobile in the medium), and then in conditions where the probability of interaction would be more limited (liposome–planar bilayer interaction). The liposome–liposome interaction producing multiple vesicle aggregation, the signal measured by DLS could be high, but was insufficient to get an insight into the kinetics of the interaction process or to monitor the changes in the organization of the system when the conditions were changed, as was allowed by QCM-D. The two systems were thus complementary.

In the liposome–liposome interaction experiment, liposomes bearing Con A as well as those bearing glycoconjugated porphyrins were in suspension in the bulk. This experiment allowed discrimination of the porphyrin derivatives depending on the presence or absence of sugar moieties. It confirmed that liposomes could be used as carriers for the studied compounds as previously suggested [43], because the glycodendrimeric porphyrins were embedded in the liposome bilayer with their glycodendrimeric arm exposed outward at the liposome surface, allowing recognition by the receptor.

These results could appear much less significant *in vivo*, where cells are not free in suspension. Using the QCM-D, we have shown that only mannosylated porphyrins borne by DMPC liposomes were strongly bound to the Con A-conjugated supported bilayer, although the Con A density on the bilayer surface was much lower than that in our previous study, where there was full coverage of the sensor surface [43]. In the present study, the Con A surface density could not exceed 35%. If the recognition process worked well for both mannosylated dendrimeric porphyrins, discrimination between compound 1 and compound 2 was more delicate, as also inferred from the DLS experiments. This could be due to the fact that the difference in the spacer length in the two porphyrins was only one ethylene oxide group, insignificant when the lectins were exposed at low density at the biomimetic membrane surface. There was enough space for mannose moieties to reach the lectin-binding site, without a long spacer. The situation was different when lectin molecules were grafted at high density and covered the entire sensor surface [43]. Con

A molecules were closer to each other, and the longer spacer in compound 2 could allow cross-linking of lectin molecules at the surface, strengthening porphyrin attachment to them.

The specificity of the lectin–porphyrin interaction had a predominant effect in the overall interaction. The comparison of the results in Figs. 6 and 7 shows that this specific interaction not only would drive the porphyrins toward their target, but also that it would allow porphyrin persistence at the cell surface, and could eventually favour its penetration into the membrane. A recent analysis by fluorescence measurements [74] has shown that compared to other series of tetraphenylporphyrin derivatives, dendrimeric compounds were able to penetrate deeper into a liposome bilayer. However within the dendrimeric porphyrin series, despite the stronger non-specific interaction with a monolayer of the glycoconjugated porphyrins compared to the non-glycoconjugated one, fluorescence quenching did not show any significant difference in penetration depth between the three compounds 1c, 1 and 2 when Con A was absent [42]. Conversely, with respect to the specific interaction, both compounds 1 and 2 proved to be interesting molecules.

## 5. Conclusion

The glycodendrimeric porphyrins borne by DMPC liposomes proved to interact specifically with Con A grafted on a retinoblastoma biomimetic membrane model. No effect of the spacer length on the interaction has been observed between compound 1 and compound 2 for the two studied systems (liposomes and supported planar bilayer). The specific interaction appeared to be crucial to the overall interaction with the biomimetic membrane since only liposomes bearing mannosylated porphyrins were able to bind to the membrane model surface. Their evaluation on the retinoblastoma Y79 cell line is currently in progress to confirm their activity as well as the relevance of our biomimetic membrane model. Added to our previous results, which showed that the sugar moieties of the glycoconjugated dendrimeric porphyrins favoured their non-specific interaction with phospholipids-cholesterol model membranes compared to compound 1c as well as their specific interaction with Con A (free or immobilized on SAM surface), the glycodendrimeric porphyrins appear as very promising drugs.

## Acknowledgments

The authors acknowledge the financial support of A. Makky's PhD by ARC (Association pour la Recherche contre le Cancer). The authors also wish to thank Professor Udo Bakowsky (Department of

Pharmaceutical Technology and Biopharmacy, Philipps-Universität, Marburg, Germany) for helpful discussions and advices on the Con A coupling methods.

## References

- [1] D.E. Dolmans, D. Fukumura, R.K. Jain, Photodynamic therapy for cancer, *Nat. Rev. Cancer* 3 (2003) 380–387.
- [2] H. Stephan, R. Boeloeni, A. Eggert, N. Bornfeld, A. Schueler, Photodynamic therapy in retinoblastoma: effects of verteporfin on retinoblastoma cell lines, *Invest. Ophthalmol. Vis. Sci.* 49 (2008) 3158–3163.
- [3] M. Lupu, C.D. Thomas, Ph. Maillard, B. Loock, B. Chauvin, I. Aerts, A. Croisy, E. Belloir, A. Volk, J. Mispelter, Na-23 MRI longitudinal follow-up of PDT in a xenograft model of human retinoblastoma, *Photodiag. Photodyn. Ther.* 6 (2009) 214–220.
- [4] P. Maillard, M. Lupu, C.D. Thomas, J. Mispelter, Vers un nouveau traitement du rétinoblastome? *Ann. Pharm. Fr.* 68 (2010) 195–202.
- [5] I. Aerts, P. Leuraud, J. Blais, A.-L. Pouliquen, Ph. Maillard, C. Houdayer, J. Couturier, X. (in press), Sastre-Garau, F. Doz, M.-F. Poupon, In vivo efficacy of photodynamic therapy in three new xenograft models of human retinoblastoma, *Photodiag. Photodyn. Ther.* 7 (2010) 275–283.
- [6] R. van Hillegersberg, W.J. Kort, J.H. Wilson, Current status of photodynamic therapy in oncology, *Drugs* 48 (1994) 510–527.
- [7] T.J. Dougherty, C.J. Gomer, B.W. Henderson, G. Jori, D. Kessel, M. Korbekij, J. Moan, Q. Peng, Photodynamic therapy, *J. Natl Cancer Inst.* 90 (1998) 889–905.
- [8] R. Bonnett, Photosensitizers of the porphyrin and phthalocyanine series for photodynamic therapy, *Chem. Soc. Rev.* 24 (1995) 19–33.
- [9] R.F. Pasternack, P.R. Huber, P. Boyd, G. Engasser, L. Francesconi, E. Gibbs, P. Fasella, G. Cerio Ventura, L.D. Hinds, Aggregation of meso-substituted water-soluble porphyrins, *JACS* 94 (1972) 4511–4517.
- [10] G. Csik, E. Balog, I. Voszka, F. Tölgyesi, D. Oulmi, P. Maillard, M. Momenteau, Glycosylated derivatives of tetraphenyl porphyrin: photophysical characterization, self-aggregation and membrane binding, *J. Photochem. Photobiol. B Biol.* 44 (1998) 216–224.
- [11] D. Oulmi, P. Maillard, C. Vever-Bizet, M. Momenteau, D. Brault, Glycosylated porphyrins: characterization of association in aqueous solutions by absorption and fluorescence spectroscopies and determination of singlet oxygen yield in organic media, *Photochem. Photobiol.* 67 (1998) 511–518.
- [12] M. Momenteau, P. Maillard, M.A. De Belinay, D. Carrez, A. Croisy, Tetrapyrrolic glycosylated macrocycles for an application in PDT, *J. Biomed. Opt.* 4 (1999) 298–318.
- [13] I. Laville, T. Figueiredo, B. Loock, S. Pigaglio, Ph. Maillard, D.S. Grierson, D. Carrez, A. Croisy, J. Blais, Synthesis, cellular internalization and photodynamic activity of glucosylated derivatives of tri and tetra(meta-hydroxyphenyl)chlorins, *Bioorg. Med. Chem.* 11 (2003) 1643–1652.
- [14] I. Laville, S. Pigaglio, J.C. Blais, B. Loock, Ph. Maillard, D.S. Grierson, J. Blais, A study of the stability of tri(glucosyloxyphenyl)chlorin, a sensitizer for photodynamic therapy, in human colon tumour cells: a liquid chromatography and MALDI-TOF mass spectrometry analysis, *Bioorg. Med. Chem.* 12 (2004) 3673–3682.
- [15] I. Laville, S. Pigaglio, J.C. Blais, F. Doz, B. Loock, Ph. Maillard, D.S. Grierson, J. Blais, Photodynamic efficiency of diethylene glycol-linked glycoconjugated porphyrins in human retinoblastoma cells, *J. Med. Chem.* 49 (2006) 2558–2567.
- [16] P. Maillard, B. Loock, D.S. Grierson, I. Laville, J. Blais, F. Doz, L. Desjardins, D. Carrez, J.L. Guerquin-Kern, A. Croisy, In vitro phototoxicity of glycoconjugated porphyrins and chlorins in colorectal adenocarcinoma (HT29) and retinoblastoma (Y79) cell lines, *Photodiag. Photodyn. Ther.* 4 (2007) 261–268.
- [17] X. Chen, C.M. Drain, Photodynamic therapy using carbohydrate conjugated porphyrins, *Drug Des. Rev. Online* 1 (2004) 215–234.
- [18] J. Cavaleiro, J. Tomé, M. Faustino, Synthesis of glycoporphyrins, in: E. El Ashry (Ed.), *Heterocycles from carbohydrate precursors*, vol. 7, Springer, Berlin/Heidelberg, 2007, pp. 179–248.
- [19] X. Zheng, R.K. Pandey, Porphyrin-carbohydrate conjugates: impact of carbohydrate moieties in photodynamic therapy (PDT), *Anti Canc. Agents Med. Chem.* 8 (2008) 241–268.
- [20] M. Monsigny, A.C. Roche, P. Midoux, Endogenous lectins and drug targeting, *Ann. NY Acad. Sci.* 551 (1988) 399–413, discussion 413–394.
- [21] R. Lotan, A. Raz, Lectins in cancer cells, *Ann. NY Acad. Sci.* 551 (1988) 385–398.
- [22] S. Ballut, A. Makky, B. Loock, J.P. Michel, Ph. Maillard, V. Rosilio, New strategy for targeting of photosensitizers. Synthesis of glycodendrimeric phenylporphyrins, incorporation into a liposome membrane and interaction with a specific lectin, *Chem. Commun.* (2009) 224–226.
- [23] S. Giegel, M.F. Rajewsky, T. Ciesiolka, H.J. Gabius, Endogenous sugar receptor (lectin) profiles of human retinoblastoma and retinoblast cell lines analyzed by cytological markers, affinity chromatography and neoglycoprotein-targeted photolysis, *Anticancer Res.* 9 (1989) 723–730.
- [24] S. Ballut, B. Loock, Ph. Maillard, New strategy for the targeting of photosensitizers. Synthesis, characterisation and photobiological property of porphyrins bearing glycodendrimeric moieties, *J. Org. Chem.* accepted.
- [25] J. Spikes, G. Jori, Photodynamic therapy of tumours and other diseases using porphyrins, *Laser Med. Sci.* 2 (1987) 3–15.
- [26] M.C. Desroches, A. Kasselouri, M. Meyniel, P. Fontaine, M. Goldmann, P. Prognon, Ph. Maillard, V. Rosilio, Incorporation of glycoconjugated porphyrin derivatives into phospholipid monolayers: a screening method for the evaluation of their interaction with a cell membrane, *Langmuir* 20 (2004) 11698–11705.
- [27] A.A. Hidalgo, M. Tabak, O.N. Oliveira Jr., The interaction of meso-tetraphenylporphyrin with phospholipid monolayers, *Chem. Phys. Lipids* 134 (2005) 97–108.
- [28] F. Ricchelli, G. Jori, Distribution of porphyrins in the various compartments of unilamellar liposomes of dipalmitoyl-phosphatidylcholine as probed by fluorescence spectroscopy, *Photochem. Photobiol.* 44 (1986) 151–157.
- [29] M. Hoebeke, The importance of liposomes as models and tools in the understanding of photosensitization mechanisms, *J. Photochem. Photobiol. B Biol.* 28 (1995) 189–196.
- [30] F. Ricchelli, Photophysical properties of porphyrins in biological membranes, *J. Photochem. Photobiol. B Biol.* 29 (1995) 109–118.
- [31] F. Ricchelli, S. Gobbo, G. Moreno, C. Salet, L. Brancalione, A. Mazzini, Photophysical properties of porphyrin planar aggregates in liposomes, *Eur. J. Biochem.* 253 (1998) 760–765.
- [32] D. Brault, Physical chemistry of porphyrins and their interactions with membranes: the importance of pH, *J. Photochem. Photobiol. B Biol.* 6 (1990) 79–86.
- [33] K. Kuzelova, D. Brault, Interactions of dicarboxylic porphyrins with unilamellar lipidic vesicles: drastic effects of pH and cholesterol on kinetics, *Biochemistry* 34 (1995) 11245–11255.
- [34] N. Maman, D. Brault, Kinetics of the interactions of a dicarboxylic porphyrin with unilamellar lipidic vesicles: interplay between bilayer thickness and pH in rate control, *Biochim. Biophys. Acta Biomembr.* 1414 (1998) 31–42.
- [35] B. Ehrenberg, E. Gross, The effect of liposomes membrane composition on the binding of the photosensitizers HPD and PHOTOFRIN II, *Photochem. Photobiol.* 48 (1988) 461–466.
- [36] E. Gross, B. Ehrenberg, The partition and distribution of porphyrins in liposomal membranes. A spectroscopic study, *Biochim. Biophys. Acta Biomembr.* 983 (1989) 118–122.
- [37] A. Lavi, H. Weitman, R.T. Holmes, K.M. Smith, B. Ehrenberg, The depth of porphyrin in a membrane and the membrane's physical properties affect the photosensitizing efficiency, *Biophys. J.* 82 (2002) 2101–2110.
- [38] A.J. Fiesler, R.E. Anderson, Chemistry and metabolism of lipids in the vertebrate retina, *Prog. Lipid Res.* 22 (1983) 79–131.
- [39] D. Huster, K. Arnold, K. Gawrisch, Influence of docosahexaenoic acid and cholesterol on lateral lipid organization in phospholipid mixtures, *Biochemistry* 37 (1998) 17299–17308.
- [40] D. Huster, K. Arnold, K. Gawrisch, Strength of Ca<sup>2+</sup> binding to retinal lipid membranes: consequences for lipid organization, *Biophys. J.* 78 (2000) 3011–3018.
- [41] M.A. Yorek, P.H. Figard, T.L. Kaduce, A.A. Spector, A comparison of lipid metabolism in two human retinoblastoma cell lines, *Invest. Ophthalmol. Vis. Sci.* 26 (1985) 1148–1154.
- [42] A. Makky, J.P. Michel, S. Ballut, A. Kasselouri, Ph. Maillard, V. Rosilio, Effect of cholesterol and sugar on the penetration of glycodendrimeric phenylporphyrins into biomimetic models of retinoblastoma cells membranes, *Langmuir* 26 (2010) 11145–11156.
- [43] A. Makky, J.P. Michel, A. Kasselouri, E. Briand, Ph. Maillard, V. Rosilio, Evaluation of the specific interactions between glycodendrimeric porphyrins, free or incorporated into liposomes, and concanavalin A by fluorescence spectroscopy, surface pressure, and QCM-D measurements, *Langmuir* 26 (2010) 12761–12768.
- [44] S. Mordon, J.M. Devoisselle, S. Soulié, Fluorescence spectroscopy of pH in vivo using a dual-emission fluorophore (C-SNAFL-1), *J. Photochem. Photobiol. B Biol.* 28 (1995) 19–23.
- [45] A.D. Bangham, M.M. Standish, J.C. Watkins, Diffusion of univalent ions across the lamellae of swollen phospholipids, *J. Mol. Biol.* 13 (1965) 238–252, IN226-IN227.
- [46] V. Faivre, V. Rosilio, P. Boullanger, L. Martins Almeida, A. Baszkin, Fucosylated neoglycolipids: synthesis and interaction with a phospholipid, *Chem. Phys. Lipids* 109 (2001) 91–101.
- [47] V. Faivre, M.L. Costa, P. Boullanger, A. Baszkin, V. Rosilio, Specific interaction of lectins with liposomes and monolayers bearing neoglycolipids, *Chem. Phys. Lipids* 125 (2003) 147–159.
- [48] J.N. Sanders, S.A. Chenoweth, F.P. Schwarz, Effect of metal ion substitutions in concanavalin A on the binding of carbohydrates and on thermal stability, *J. Inorg. Biochem.* 70 (1998) 71–82.
- [49] Y. Nakano, M. Mori, S. Nishinohara, Y. Takita, S. Naito, H. Kato, M. Taneichi, K. Komuro, T. Uchida, Surface-linked liposomal antigen induces IgE-selective unresponsiveness regardless of the lipid components of liposomes, *Bioconj. Chem.* 12 (2001) 391–395.
- [50] G. Liu, Y. Lin, Nanomaterial labels in electrochemical immunosensors and immunoassays, *Talanta* 74 (2007) 308–317.
- [51] H. Chen, V. Torchilin, R. Langer, Lectin-bearing polymerized liposomes as potential oral vaccine carriers, *Pharm. Res.* 13 (1996) 1378–1383.
- [52] J.W. Becker, G.N. Reeke Jr., J.L. Wang, B.A. Cunningham, G.M. Edelman, The covalent and three-dimensional structure of concanavalin A. III. Structure of the monomer and its interactions with metals and saccharides, *J. Biol. Chem.* 250 (1975) 1513–1524.
- [53] H.M.L.R. Santos, F.B. de Queiroz, R.M.S. Maior, S.C. do Nascimento, N.S.S. Magalhães, Cytotoxicity of doxorubicin-loaded Con A-liposomes, *Drug Dev. Res.* 67 (2006) 430–437.
- [54] A.A. Bogdanov jr, A.L. Klivanov, V.P. Torchilin, Protein immobilization on the surface of liposomes via carbodiimide activation in the presence of N-hydroxysulfosuccinimide. New strategy for the targeting of photosensitizers. Synthesis, characterisation and photobiological property of porphyrins bearing glycodendrimeric moieties, *FEBS Lett.* 231 (1988) 381–384.
- [55] Z.V. Leonenko, A. Carnini, D.T. Cramb, Supported planar bilayer formation by vesicle fusion: the interaction of phospholipid vesicles with surfaces and the effect of gramicidin on bilayer properties using atomic force microscopy, *Biochim. Biophys. Acta Biomembr.* 1509 (2000) 131–147.

- [56] E. Kalb, J. Engel, L.K. Tamm, Binding of proteins to specific target sites in membranes measured by total internal reflection fluorescence microscopy, *Biochemistry* 29 (1990) 1607–1613.
- [57] M. Grandbois, H. Clausen-Schaumann, H. Gaub, Atomic force microscope imaging of phospholipid bilayer degradation by phospholipase A2, *Biophys. J.* 74 (1998) 2398–2404.
- [58] M. Ross, C. Steinem, H.J. Galla, A. Janshoff, Visualization of chemical and physical properties of calcium-induced domains in DPPC/DPPS Langmuir–Blodgett layers, *Langmuir* 17 (2001) 2437–2445.
- [59] C.A. Keller, B. Kasemo, Surface specific kinetics of lipid vesicle adsorption measured with a quartz crystal microbalance, *Biophys. J.* 75 (1998) 1397–1402.
- [60] C. Steinem, A. Janshoff, W.P. Ulrich, M. Sieber, H.J. Galla, Impedance analysis of supported lipid bilayer membranes: a scrutiny of different preparation techniques, *Biochim. Biophys. Acta Biomembr.* 1279 (1996) 169–180.
- [61] E. Reimhult, F. Höök, B. Kasemo, Intact vesicle adsorption and supported biomembrane formation from vesicles in solution: influence of surface chemistry, vesicle size, temperature, and osmotic pressure, *Langmuir* 19 (2002) 1681–1691.
- [62] E. Reimhult, F. Höök, B. Kasemo, Vesicle adsorption on SiO<sub>2</sub> and TiO<sub>2</sub>: dependence on vesicle size, *J. Chem. Phys.* 117 (2002) 7401–7405.
- [63] T.E. Starr, N.L. Thompson, Formation and characterization of planar phospholipid bilayers supported on TiO<sub>2</sub> and SrTiO<sub>3</sub> single crystals, *Langmuir* 16 (2000) 10301–10308.
- [64] R. Richter, A. Mukhopadhyay, A. Brisson, Pathways of lipid vesicle deposition on solid surfaces: a combined QCM-D and AFM study, *Biophys. J.* 85 (2003) 3035–3047.
- [65] B. Seantier, C. Breffa, O. Felix, G. Decher, Dissipation-enhanced quartz crystal microbalance studies on the experimental parameters controlling the formation of supported lipid bilayers, *J. Phys. Chem. B* 109 (2005) 21755–21765.
- [66] R.P. Richter, R. Bérat, Alain R. Brisson, Formation of solid-supported lipid bilayers: an integrated view, *Langmuir* 22 (2006) 3497–3505.
- [67] E. Reimhult, M. Zach, F. Hook, B. Kasemo, A multitechnique study of liposome adsorption on Au and lipid bilayer formation on SiO<sub>2</sub>, *Langmuir* 22 (2006) 3313–3319.
- [68] A.R. Patel, C.W. Frank, Quantitative analysis of tethered vesicle assemblies by quartz crystal microbalance with dissipation monitoring: binding dynamics and bound water content, *Langmuir* 22 (2006) 7587–7599.
- [69] H. Brochu, P. Vermette, Liposome layers characterized by quartz crystal microbalance measurements and multirelease delivery, *Langmuir* 23 (2007) 7679–7686.
- [70] F. Hook, B. Kasemo, T. Nylander, C. Fant, K. Sott, H. Elwing, Variations in coupled water, viscoelastic properties, and film thickness of a Mefp-1 protein film during adsorption and cross-linking: a quartz crystal microbalance with dissipation monitoring, ellipsometry, and surface plasmon resonance study, *Anal. Chem.* 73 (2001) 5796–5804.
- [71] A.K. Dutta, A. Nayak, G. Belfort, Viscoelastic properties of adsorbed and cross-linked polypeptide and protein layers at a solid–liquid interface, *J. Colloid Interface Sci.* 324 (2008) 55–60.
- [72] J.J. Ramsden, Biomimetic protein immobilization using lipid bilayers, *Biosens. Bioelectron.* 13 (1998) 593–598.
- [73] P. Calvez, S. Bussières, E. Demers, C. Salesse, Parameters modulating the maximum insertion pressure of proteins and peptides in lipid monolayers, *Biochimie* 91 (2009) 718–733.
- [74] H. Ibrahim, A. Kasselouri, C. You, Ph. Maillard, V. Rosilio, R. Pansu, P. Prognon, Glycoconjugated porphyrins usable in photodynamic therapy: self-aggregation, association with albumin, and localisation in DMPC liposomes as a simplified cell membrane model, *J. Photochem. Photobiol. Chem.* (2010), doi:10.1016/j.jphotochem.2010.09.008.